

Decay of excited nuclei produced in the $^{78,82}\text{Kr}+^{40}\text{Ca}$ reactions at 5.5 MeV/nucleon

G. Ademard, J.P. Wieleczo, J. Gomez del Campo, M. Lacommar, E. Bonnet, M. Vigilante, A. Chbihi, J.D. Frankland, E. Rosato, G. Spadaccini, et al.

► **To cite this version:**

G. Ademard, J.P. Wieleczo, J. Gomez del Campo, M. Lacommar, E. Bonnet, et al.. Decay of excited nuclei produced in the $^{78,82}\text{Kr}+^{40}\text{Ca}$ reactions at 5.5 MeV/nucleon. 5th International Conference FUSSION11, May 2011, Saint Malo, France. pp.10005, 10.1051/epjconf/20111710005 . in2p3-00634937

HAL Id: in2p3-00634937

<http://hal.in2p3.fr/in2p3-00634937>

Submitted on 25 Oct 2011

HAL is a multi-disciplinary open access archive for the deposit and dissemination of scientific research documents, whether they are published or not. The documents may come from teaching and research institutions in France or abroad, or from public or private research centers.

L'archive ouverte pluridisciplinaire **HAL**, est destinée au dépôt et à la diffusion de documents scientifiques de niveau recherche, publiés ou non, émanant des établissements d'enseignement et de recherche français ou étrangers, des laboratoires publics ou privés.

Decay of excited nuclei produced in the $^{78,82}\text{Kr} + ^{40}\text{Ca}$ reactions at 5.5 MeV/nucleon

G. Ademard^{1,a}, J.P. Wieleczko¹, J. Gomez del Campo², M. LaCommara^{3,4}, E. Bonnet¹, M. Vigilante^{3,4}, A. Chbihi¹, J.D. Frankland¹, E. Rosato^{3,4}, G. Spadaccini^{3,4}, Sh.A. Kalandarov^{5,6}, C. Beck⁷, S. Barlini⁸, B. Borderie⁹, R. Bougault¹⁰, R. Dayras¹¹, G. De Angelis¹², J. De Sanctis¹³, V.L. Kravchuk¹², P. Lautesse¹⁴, N. Le Neindre¹⁰, J. Moisan^{1,15}, A. D'Onofrio¹⁶, M. Parlog¹⁰, D. Pierrousakou⁴, M. Romoli⁴, R. Roy¹⁵, G.G. Adamian^{5,6}, and N.V. Antonenko⁵.

- ¹ Grand Accélérateur National d'Ions Lourds (GANIL), CEA/DSM-CNRS/IN2P3, Bvd H. Becquerel, 14076, Caen, France
- ² Physics Division, Oak Ridge National Laboratory, Oak Ridge, TN 37831, USA
- ³ Dipartimento di Scienze Fisiche, Università di Napoli "Federico II", I-80126, Napoli, Italy
- ⁴ INFN, Sezione di Napoli, I-80126, Napoli, Italy
- ⁵ Joint Institute for Nuclear Research, 141980 Dubna, Russia
- ⁶ Institute of Nuclear Physics, 702132 Tashkent, Uzbekistan
- ⁷ IPHC, IN2P3-CNRS and Université Strasbourg, F-67037, Strasbourg Cedex2, France
- ⁸ INFN, Sezione di Firenze, I-50125 Firenze, Italy
- ⁹ IPNO, IN2P3-CNRS and Université Paris-Sud 11, F-91406, Orsay Cedex, France
- ¹⁰ LPC, IN2P3-CNRS, ENSICAEN and Université, F-14050, Caen Cedex, France
- ¹¹ CEA, IRFU, SPHN, CEA/Saclay, F-91191, Gif-sur-Yvette Cedex, France
- ¹² INFN, LNL, I-35020 Legnaro (Padova) Italy
- ¹³ INFN, Sezione di Bologna, I-40127 Bologna, Italy
- ¹⁴ IPNL, IN2P3-CNRS et Université, F-69622, Villeurbanne Cedex, France
- ¹⁵ Laboratoire de Physique Nucléaire, Université de Laval, Québec, Canada
- ¹⁶ Dipartimento di Scienze Ambientali, Seconda Università di Napoli, I-81100, Caserta, Italy

Abstract. Decay modes of excited nuclei are studied in $^{78,82}\text{Kr} + ^{40}\text{Ca}$ reactions at 5.5 MeV/nucleon by means of light-charged particles measured in coincidence with intermediate mass fragments and fission-like fragments. Inclusive cross-section distributions of fragments with charge $3 \leq Z \leq 28$ are bell-shaped and a strong odd-even-staggering (o-e-s) is observed for $3 \leq Z \leq 12$. Coincidence measurements suggest that the light partners in very asymmetric fission are emitted at excitation energies below the particle emission thresholds. Data were confronted to the predictions of statistical models describing the decay of compound nuclei by emission of light particles and fragments. Comparison with models suggests that the o-e-s of the light-fragment yields is mainly due to the successive steps of compound nucleus disintegration.

1 Introduction

Evaporation of light particles and fission processes have been studied for many decades to understand thermal and collective properties of excited compound nuclei and to extract fundamental nuclear quantities like level density and fission barriers. As an example of macroscopic ingredient needed to describe the decay modes of nuclei, the mass (charge)-asymmetry degree of freedom plays a crucial role in the emission of the so-called intermediate mass fragments leading to the population of the whole mass (charge) range from evaporated particles to symmetric fission [1–3]. In a recent experiment performed at the GANIL facility, we have observed such a distribution in $^{78,82}\text{Kr} + ^{40}\text{Ca}$ reactions at 5.5 MeV/nucleon [4]. The kinetic-energy spectra and the angular distributions of fragments $3 \leq Z \leq 28$

indicate a high degree of relaxation. The inclusive cross-sections σ_Z of fragments with charge $3 \leq Z \leq 28$ are shown in Fig. 1 for the $^{78}\text{Kr} + ^{40}\text{Ca}$ (solid squares) and $^{82}\text{Kr} + ^{40}\text{Ca}$ (open squares) reactions. The σ_Z distributions for both systems exhibit a maximum around $Z = 26$. Such a shape shows that these elements come either from the symmetric fission of CN or from dissipative collisions in which the initial mass-asymmetry has been strongly relaxed. Moreover, except for $3 \leq Z \leq 5$, σ_Z measured in the $^{82}\text{Kr} + ^{40}\text{Ca}$ system is systematically lower and the yields around the symmetric fragmentation are about 25% smaller for the system having the highest neutron-to-proton ratio. Interestingly, we observe a strong odd-even-staggering (o-e-s) of the cross-sections for fragments with atomic number $Z \leq 10$. This o-e-s is also present for $Z \geq 12$ with a smaller amplitude. As shown in Fig. 1, the staggering of the yields of light fragments is very similar to the one ob-

^a e-mail: ademard@ganil.fr

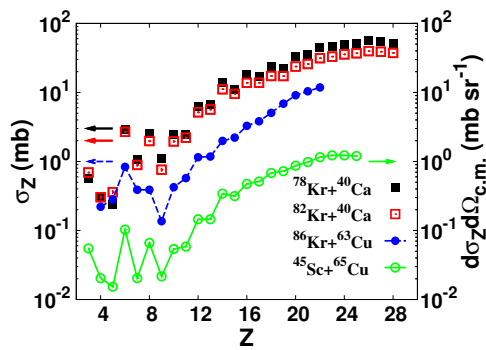


Fig. 1. Experimental cross-sections for fragments emitted in the $^{78}\text{Kr} + ^{40}\text{Ca}$ (full squares) reaction at 5.5 MeV/nucleon [4], $^{82}\text{Kr} + ^{40}\text{Ca}$ (open squares) reactions at 5.5 MeV/nucleon [4], $^{86}\text{Kr} + ^{63}\text{Cu}$ (full circles) reaction at 5.65 MeV/nucleon [6], and differential cross-section for $^{45}\text{Sc} + ^{65}\text{Cu}$ (open circles) reaction at 4.5 MeV/nucleon [5].

served for neighbouring systems as for example $^{86}\text{Kr} + ^{63}\text{Cu}$ (full circles) reaction at 5.65 MeV/nucleon or $^{45}\text{Sc} + ^{65}\text{Cu}$ (open circles) reaction at 4.5 MeV/nucleon [5,6]. Indeed the charge distributions for all reactions develop an half bell-like shape with a change of behaviour around $Z = 10$. This common feature would indicate that the o-e-s is not driven by some microscopic properties of the complementary partners of the observed light fragments since they are different in each studied reaction. A possible explanation of the staggering of the cross-sections would be that the fragments are ejected with excitation energies below the emission thresholds, otherwise the subsequent decay by light-particle emission would have blurred the fluctuations of σ_Z . Investigation of this scenario requires to study the characteristics of the emitted light particles. Indeed, coincidence measurements between light-charged particles and fragments have played a crucial role in understanding important aspects of the fragmentation process as the sharing of the excitation energies between both partners or viscosity phenomenon. In this contribution we present an event-by-event analysis of the light-charged particles (LCPs) in coincidence with fragments in order to get more insights on the emission of intermediate mass fragment in $^{78,82}\text{Kr} + ^{40}\text{Ca}$ reactions at 5.5 MeV/nucleon.

2 Experimental results

Data were collected on an even-by-event basis thanks to the high capabilities of the 4π INDRA apparatus. In a typical event associated to a binary fission, one of the partner is generally detected as well as the LCPs emitted by both partners and possibly by the composite fissioning system. Due to the low excitation energy available in the reaction, we expect a small amount of emitted particles. Consequently, the kick induced by these particles on residual fragment should be small and it is reasonable to assume that final fragments left after the secondary stage are flying back-to-back in the center-of-mass. Thus, the emission direction of one detected fragment defines the recoil di-

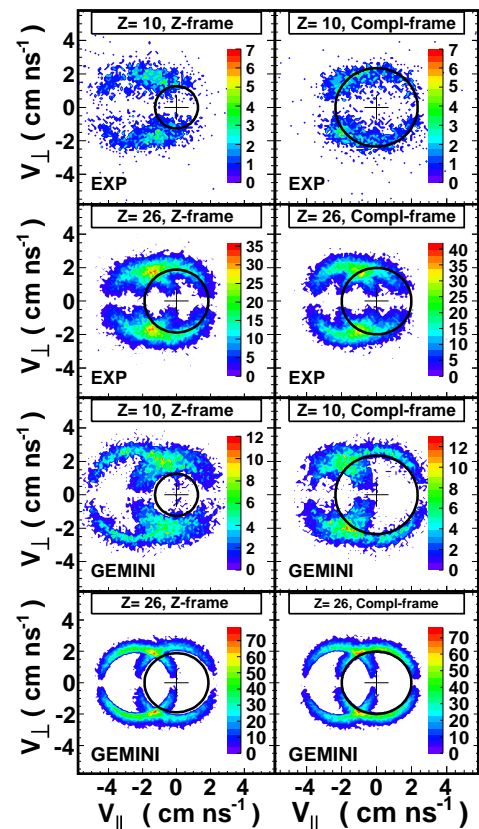


Fig. 2. Experimental and theoretical V_{\parallel} - V_{\perp} diagrams of α -particles in coincidence with Ne (first and third row) and Fe (second and fourth row) fragments. The velocities are calculated in the reference frames of the light fragment (left panels) and of the complementary fragment (right panels). Data (results of calculations) are reported in first and second (third and fourth) row, respectively. Calculations were performed with the statistical model GEMINI.

rection of its complementary partner. In the present analysis, we calculated for each fragment the relative velocity between that fragment and each detected LCP of the event. Then we consider a new frame built as follows: one axis is the direction of the fragment velocity in the c.m. frame; the plane perpendicular to this axis complete the reference frame. The relative velocities previously calculated are projected onto this new frame. Finally, we obtained the component parallel (V_{\parallel}) and perpendicular (V_{\perp}) with respect to the direction of the fragment velocity in the c.m. frame. In doing so, for fragments of a given Z emitted at different angles in the c.m., the procedure enables to define a common frame for the LCPs in coincidence with these fragments. With such a procedure applied to an ensemble of reactions, the particles emitted by one fragment of a given Z with a constant velocity value will draw one circle centered at the origin of the reference frame in a V_{\parallel} - V_{\perp} plot.

In the following we report the results on the coincidences between α -particles and fragments. The analysis with proton (not shown here) leads to similar conclusions.

Fig. 2 presents typical examples of $V_{\parallel} - V_{\perp}$ diagrams for α -Ne (first row) and α -Fe (second row) coincidences measured in the $^{78}\text{Kr} + ^{40}\text{Ca}$ reaction. The black circles represent the average velocities of emitted α -particles taken from [7]. In case of asymmetric fragmentation, as α -Ne, the relative velocities of the particles fill-in a region akin of a Coulomb ring which is centered at the origin when they are projected into the frame (termed as Compl-frame) of the complementary partner of the Ne nuclei (top right panel). On the contrary, no such a pattern can be seen when the relative velocities are plotted in the frame (termed as Z-frame) of the light partner (top left panel). For almost symmetric fragmentation, as α -Fe, both fragments emit light-particles as illustrated by the two circles centered at both reference frames. A change of behaviour is observed in the light-particle emission from asymmetric ($Z = 10$) to almost symmetric ($Z = 26$) fragmentation. The $V_{\parallel} - V_{\perp}$ diagrams for coincidences between α and $Z \leq 10$ show the same feature as the one observed from the α -Ne coincidences. Thus, in $^{78}\text{Kr} + ^{40}\text{Ca}$ reactions at 5.5 MeV/nucleon, in the case of symmetric fragmentation both fragments emit LCPs, while for a asymmetric fragmentation, only the heavy fragment emits particles. Obviously, the neutron channel should be considered but it could not be measured by our apparatus. Nevertheless, we have checked that for light fragments the energy thresholds for neutron emission are higher than for LCPs. Consequently, from this analysis, we conclude that the light fragments are produced at excitation energies below the proton or alpha emission thresholds.

3 Discussion

In this section, we compared the previous experimental features with the predictions of theoretical approaches. A global understanding of the many aspects of the compound nuclei decay modes is very challenging and calculations depends on various parameters which could be fixed by confrontation to a variety of experimental observables. Our basic strategy for the present work is to use the predictions of the model as guideline and we adopted standard values of the parameters. A fine tuning of the ingredients would not have a strong impact on our conclusions. The statistical-model code GEMINI describes the light particles and fragment emission by combining the transition-state and Hauser-Feschbach formalisms [3]. The barriers for fragment emission ($Z \geq 3$) are calculated in the framework of the finite-range liquid-drop model [8].

The thin line in Fig. 3 represents the predictions of GEMINI for the disintegration of ^{118}Ba nucleus assuming a sharp cut-off distribution of the angular momentum with $J_{max} = 69$ which is the angular momentum for which the fission barrier disappears. We assume a level-density parameter $a = A/8 \text{ MeV}^{-1}$. The shape of the Z -distribution for $12 \leq Z \leq 28$ is reasonably reproduced, although σ_Z for $18 \leq Z \leq 26$ are underestimated by roughly 20%. More dramatically, the model overestimates by about a factor 10 the integral of the σ_Z cross-sections for $3 \leq Z \leq 11$, the difference coming mainly from the very high Li cross-section, while C and O yields are larger by about a factor

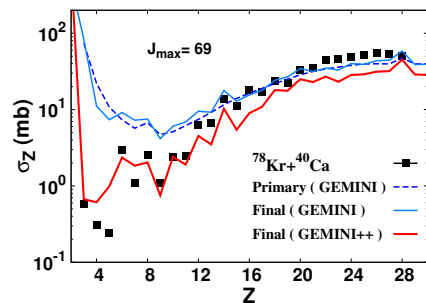


Fig. 3. Experimental cross-sections for final products emitted in the $^{78}\text{Kr} + ^{40}\text{Ca}$ reaction (full squares), compared to the predictions of the GEMINI code for final products (thin line) and primary fragments before the secondary decay by light-particle emissions (dashed line). Calculations were performed assuming a sharp cut-off distribution with $J_{max} = 69$, and a level-density parameter $a=A/8 \text{ MeV}^{-1}$. Thick line represents calculations performed with the GEMINI++ code taking standard values: $k_0 = 7.3 \text{ MeV}$, $k_{\infty} = 12 \text{ MeV}$, $a_k = 0.00517$, $c_k = 0.0345$, $a_f/a_n = 1.036$, $w = 1 \text{ fm}$, the Bohr-Wheeler decay width and including IMF emissions. We used the same notations as in [10].

3. This result does not depend on the sharp cut-off approximation and no major influence is observed by changing the level-density parameter. Finally, the magnitude of the odd-even effect is not at all reproduced for the light fragments. A low barrier for mass-asymmetric fission could explain these features of the Z -distributions for light fragments. For medium-mass nuclei as ^{118}Ba , the total kinetic energy of the fragments is tightly related to the barrier and from the energy balance, a lower potential energy would correspond to higher excitation energy in the primary fragments. From the calculations, we extracted the primary Z -distribution before secondary decays (dashed line in Fig. 3) and we observe a smooth behaviour of the Z -distribution. Thus, the initial shape of the distribution is modified by secondary emission of light-charged particles which induces the fluctuations of the yields.

It would be interesting to incorporate into the transition state formalism other potential-energy surfaces which might have a better behaviour at large mass-asymmetry than Sierk's barriers [9]. A new version of the previous code has been recently developed [10] to cope with this question of the overestimation of the light-fragment yields and wide fission-fragment mass distributions. In GEMINI++, the Rusanov's systematics [11] of fission-fragment mass distributions has been used. The mass distribution is assumed to have a Gaussian-shape with a variance linked to the stiffness of the potential energy around symmetry. The phenomenological potential energy has a larger curvature at symmetry than Sierk's predictions. Once implemented in the calculation of the fission decay width it gives a narrower fission-fragment mass distribution. The result of the calculations is represented by a thick line in Fig. 3. The improvement with respect to the predictions of the GEMINI code is spectacular. More specifically the yields and the o-e-s of the light-fragments are better reproduced with GEMINI++. Thus the main conclusion from these calculations is that the odd-even-staggering would be pre-

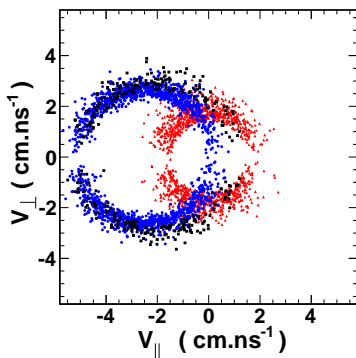


Fig. 4. $V_{\parallel} - V_{\perp}$ diagram for α -Ne deduced from the calculations with GEMINI. The various sources of α are unfolded and represented by different colors: emission correlated to the Ne fragment (red points); emission from complementary partners (blue points); and successive emission from compound nuclei (black points).

dominantly associated to the secondary emission of light-particles, since the primary Z -distribution has a Gaussian-like shape. This scenario could be easily identified by studying the coincidences between light-particles and fragments.

In the following step of the analysis we applied the coincidence method described above to the results of the calculations performed with the GEMINI code. Third and fourth row in Fig. 2 present the $V_{\parallel} - V_{\perp}$ diagram for α -Ne and α -Fe, respectively. The pattern for α -Fe is very similar to the experimental one (second row in Fig. 2) showing that the two partners emit α -particles. However, in case of α -Ne coincidences, we observe a strong accumulation of counts drawing a Coulomb ring which corresponds to the α -emission from an excited fragment leading to the observed Ne. Such a pattern strongly differs from the experimental one. In the previous calculations, we could tagged the origin of the particles emitted during a binary fission leading to a final fragment. Fig. 4 shows the result of such a tagging procedure in the $V_{\parallel} - V_{\perp}$ diagram for α -Ne coincidences obtained with GEMINI code. Here the velocities are computed in the reference of the Ne fragment. We observe three sources of emission which develop three Coulomb rings. One ring is located around the origin of the reference frame (red points in Fig. 4) and corresponds to the α -emission from a Mg fragment; The second ring (blue points) is associated to the emission from complementary partner of the light fragments leading to Ne; The third ring (black points) is associated to α -emission from compound nucleus before the fragmentation process. A careful analysis of the calculations shows that Ne fragment (and light fragments too) is mostly populated by secondary emission. The analysis performed with the outcome of GEMINI++ gives the same kind of pattern for the $V_{\parallel} - V_{\perp}$ diagram. Indeed, examination of the models indicates that the sharing of the total excitation energy left after fragmentation is the main source of the excitation energy stored in the light fragment. Thus we obtain the same pattern (not shown here) for the velocity diagram since equivalent assumptions for the sharing of the excitation energy are made in the two codes.

4 Conclusion

We have studied the light-charged particles in coincidence with fragments produced in $^{78.82}\text{Kr} + ^{40}\text{Ca}$ reactions at 5.5 MeV/nucleon. The experimental results suggest that the light fragments are emitted at excitation energies below the emission thresholds. This finding is also supported by calculations. The first conclusion is that the o-e-s of the cross-sections of the light fragments is not related to secondary emission. The second conclusion is that the σ_z of the light fragments reflect the primary fragmentation and thus they provide important constraints on the energetic balance. The level scheme of the light fragments could also play a role in the final phase space for the decay. Since even-even and odd-odd nuclei have completely different level scheme, one could expect odd-even-staggering for the yields. Moreover, the collective energy of the configuration governs the phase space left for the disintegration, this collective energy should include the properties responsible of the staggering of the yields. In a recent investigation [4] we have shown that the dinuclear system model [2] reproduces very well the observed o-e-s. In this model, the key quantity is the driving potential that contains some microscopic part which develops an odd-even effect. The amplitude of the staggering depends of the neutron content of the system and is more pronounced for neutron deficient system. Since a staggering in the driving potential will conversely correspond to a staggering in the yields, one expects the influence of the multichance emission to induce the observed feature. Further analysis within the dinuclear system model is foreseen to check this scenario with the present data and with new data obtained at higher bombarding energy [12].

References

1. L.G. Moretto and G.J. Wozniak, Prog. Part. Nucl. Phys. **21**, 401 (1988).
2. Sh.A. Kalandarov, G.G. Adamian, N.V. Antonenko, and W. Scheid, Phys. Rev. **C82**, 044603 (2010).
3. R.J. Charity *et al.*, Nucl. Phys. **A476**, 516 (1988).
4. G. Ademard *et al.*, Phys. Rev. **C83**, 054619 (2011)
5. L.G. Sobotka *et al.*, Phys. Rev. **C 36**, 2713 (1987).
6. J. Boger, J.M. Alexander, A. Elmaani, S. Kox, R.A. Lacey, A. Narayanan, D.J. Moses, M.A. McMahhan, P.A. DeYoung, and C.J. Gelderloos, Phys. Rev. **C 49**, 1597 (1994).
7. W.J. Parker *et al.*, Phys. Rev. **C 44**, 774 (1991).
8. A.J. Sierk, Phys. Rev. Lett. **55**, 582 (1985).
9. K. Mazurek, J.P. Wieleczko, C. Schmitt, G. Ademard, P.N. Nadtochy, Proceedings of the International Conference on Fusion, FUSION11, 2-6 May 2011, Saint-Malo.
10. D. Mancusi, R.J. Charity, and J. Cugnon, Phys. Rev. **C 82**, 044610 (2010)
11. A.Y. Rusanov, M.G. Itkis, and V.N. Okolovich, Phys. At. Nucl. **60**, 683 (1997).
12. S. Pirrone *et al.*, Proceedings of the International Conference on Fusion, FUSION11, 2-6 May 2011, Saint-Malo.